

# Chemiluminescent NiO\* emissions: band systems and spectral simulation

R.L. Gattinger, W.F.J. Evans, and E.J. Llewellyn

**Abstract:** Following the renewed interest in metal oxide emissions in the night airglow, high-resolution laboratory observations of NiO\* in the visible and near-infrared regions of the spectrum are reviewed, and approximate spectroscopic constants are derived to augment those already available in the literature. A preliminary spectral band simulation model is developed for the relevant NiO systems. Franck–Condon factors, calculated using the preliminary spectroscopic constants, are used in the model to conduct an iterative comparison with low-resolution NiO\* chemiluminescent emissions observed in the laboratory. Relative vibrational level populations are estimated, and shortcomings of the model are noted. The existence of a new NiO band system is also suggested.

PACS Nos: 33.20.Kf, 34.50.Ez, 92.60.H-, 92.60.hb, 92.60.hc, 92.60.hw, 95.30.Ft, 95.30.Fg, 95.30.Kr

**Résumé :** Suivant le renouveau d'intérêt pour la contribution des émissions des oxydes métalliques à la lueur nocturne de haute atmosphère, nous passons en revue les mesures en laboratoire de haute résolution du NiO\* dans le visible et le proche infrarouge et en déduisons des valeurs approximatives des constantes spectroscopiques pour améliorer les valeurs déjà disponibles dans la littérature. Nous développons un modèle préliminaire approximatif de la bande spectrale pour les systèmes NiO\* d'intérêt. Nous calculons les facteurs de Frank–Condon à partir des constantes spectroscopiques préliminaires et nous les utilisons dans le modèle pour faire une comparaison itérative avec les émissions de chimiluminescence de basse résolution du NiO\* faites en laboratoire. Nous estimons les populations relatives des niveaux de vibration et notons les faiblesses du modèle. Nous suggérons également l'existence d'un nouveau système de bandes dans le NiO.

[Traduit par la Rédaction]

## 1. Introduction

The detection of the FeO\* “orange” bands in the night airglow [1] has renewed interest in the interaction of metals of meteoric origin with atmospheric minor species, particularly mesospheric ozone. Extending the FeO\* observations, it is expected that chemiluminescent emission from NiO\* arising from



is also present in the airglow spectrum, albeit very faint, with a total exoergicity of  $266 \pm 4$  kJ/mol [2]. Meteorites typically have Ni–Fe ratios around 8% [3], but at times this ratio can be much higher [4] and suggests that atmospheric NiO\* emissions should also be detectable. Indeed, Evans et al. [2] have reported the first observations of NiO\* in the upper mesosphere and compared the atmospheric results with laboratory observations of NiO\* and with expected Ni–Fe ratios in the atmosphere. Although the temporal and spatial distributions of mesospheric Fe and Na have been investigated extensively with LIDAR (e.g., [5]), there do not appear to be any comparable LIDAR observations of Ni in the atmosphere.

The objective of the present study is to develop a spectral model of the NiO\* emission features that can be used to refine searches for the very weak NiO\* signatures in the night airglow spectrum. A similar model has been developed by Gattinger et al. [6] for FeO\* emissions. Individual vibrational band locations, spectral shapes, and relative band intensities within the relevant NiO\* electronic band systems are required to build a model spectrum. The relative vibrational populations in the excited electronic states are included as free parameters to enable simulations for both laboratory and mesospheric pressures.

This initial study is arbitrarily limited to the visible and near-infrared regions of the spectrum. At least two NiO\* band systems are known to be present in this spectral region: the NiO\* “blue” bands near 500 nm [7, 8] and the “red”  $^3\Sigma^- - X^3\Sigma^-$  system that occurs in the 620 nm region [9]. These laboratory observations are reviewed, and approximate spectroscopic constants, many currently unavailable, are derived from high spectral resolution studies. The constants are then used in an iterative manner, together with the model, to construct spectra for the band systems and to compare the predicted spectral profiles with low-resolution observations

Received 5 April 2011. Accepted 17 June 2011. Published at www.nrcresearchpress.com/cjp on 3 August 2011.

**R.L. Gattinger and E.J. Llewellyn.** ISAS, Department of Physics and Engineering Physics, 116 Science Place, University of Saskatchewan, Saskatoon, SK S7N 5E2, Canada.

**W.F.J. Evans.** NorthWest Research Associates Inc., 4118 148 Avenue N.E., Redmond, WA 98052, USA; Centre for Research in Earth and Space Science, York University, 4700 Keele Street, Toronto, ON M3J 1P3, Canada.

**Corresponding author:** E.J. Llewellyn (e-mail: edward.llewellyn@usask.ca).

**Table 1.** Molecular constants applied in the model simulations of the NiO “blue” and “red” bands.

Parameter	$X^3\Sigma^-$	Red $A^3\Sigma^-$	Blue $B^3\Sigma(?)$	Blue $C^3\Sigma(?)$	New D(?)
$T_e$	0.0	16075.0	18860.0	199650	15700.0
$\omega_e$	839.69	617.0	587.0	605.0	614.0
$\omega_e x_e$	5.73	9.5	2.6	3.0	1.0(?)
$B_0 0e$	0.46	0.430	0.390	0.390	0.52(?)
$B_0 1e$	0.53	0.452	0.475	0.475	0.52(?)
$B_0 1f$	0.52	0.450	0.485	0.485	0.52(?)
$\alpha_e$	0.0043	0.005	0.004	0.005	0.006(?)
$D_0$	$0.76 \times 10^{-6}$	$0.9 \times 10^{-6}$	$1.2 \times 10^{-6}$	$1.1 \times 10^{-6}$	$1.5 \times 10^{-6} (?)$
$\lambda_0$	25.2	-138.0	100.0	100.0	40.0(?)
$\gamma$	-0.25	-1.00	0.0(?)	0.0(?)	0.0(?)

**Note:** Except for the  $X$  state, the value of  $D_0$  is calculated from the approximate expression  $4B_0^3/\omega_e^2$  [12]. The entries followed by (?) are assumed values. The units for various molecular constants are  $\text{cm}^{-1}$ .

of the NiO\* emissions that contain information on relative band and system intensities. Differences between the modeled and observed spectra are noted, and the possible presence of previously unidentified band systems is discussed.

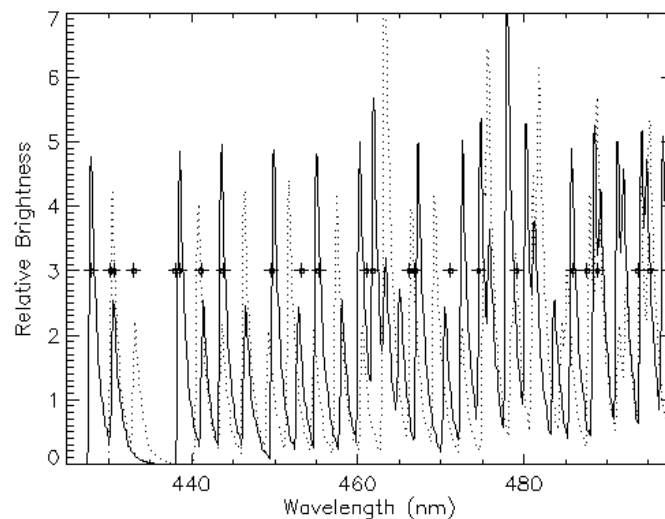
## 2. NiO\* band systems

### 2.1 Molecular constants from laboratory observations

The early laboratory spectral observations of NiO are most notably those by Rosen [10] and Malet and Rosen [11], who recorded the spectral locations of numerous bands and proposed a band system classification scheme. Subsequent observations led to the identification of the electronic ground state as an  $X^3\Sigma^-$  configuration [7, 9] with three spin states,  $0e$ ,  $1e$ , and  $1f$ , or alternatively,  $F_1$ ,  $F_2$ , and  $F_3$  [12]. For the  $X^3\Sigma^-$  state, the molecular constants obtained by Friedman-Hill and Field [9] are used in the analysis here (Table 1). The rotational constants for the three spin substates, calculated from the tabulated energy levels, are listed individually in Table 1. Transitions to the three substates from upper states with the same spin terms are used throughout the model calculations.

The upper state of the blue band system has not been definitively identified; however, according to the observations by Srdanov and Harris [7] multiple spin states are present in the upper state and the bands consist of simple red-degraded P and R branches. Balfour et al. [8] also observed only red-degraded P and R branches in the blue system. As mentioned by Balfour et al. [8], vibrational assignments in the NiO blue system remain problematic. A further example of the inconsistency of band assignments is apparent in the work of Srdanov and Harris [7] in their Table 2 where the listed values for  $\omega_e$  vary from 618 to 797  $\text{cm}^{-1}$ . In the same Table 2, Srdanov and Harris [7] identify specific spin state transitions that suggest that the blue band system is actually two very similar band systems with different wavenumber origins; their proposed band ordering is partially based on measured isotopic shifts that vary with  $\nu'$  level. The difficulty of band assignments is further exemplified by the list of observed band heads, given by Balfour et al. [8] in their Table 1, that are not well matched with a single band system. Malet and Rosen [11] concluded that there are two band systems, their

**Fig. 1.** Spectral locations of the model blue B (dot) and C (solid) bands for  $\nu'' = 0$  and  $\nu'' = 1$ , collocated with band features observed by Balfour et al. [8] (plus signs). The laboratory observations were obtained by laser-induced fluorescence and are limited to the lowest  $\nu''$  levels. Approximately 90% of the observed band locations are matched in the model to better than 0.5 nm. All band brightnesses are assumed to be equal. The brightness alternation is due to the manner in which the three spin states combine in each band.



Systems IV and V, with similar origins of 19314 and 19602  $\text{cm}^{-1}$  and with  $\omega'' = 825$  and 820  $\text{cm}^{-1}$ , respectively. Their  $\omega''$  values are in good agreement with the  $X^3\Sigma^- \omega_e$  value in Table 1, indicating that the lower state in both systems is the ground state. By postulating two band systems here, and by iteratively fitting the band locations in the model to the observed band head positions given by Balfour et al. [8], the comparison shown in Fig. 1 shows the model predicting approximately 90% of the observed band locations to within 0.5 nm. This level of wavenumber accuracy is adequate for comparison with atmospheric spectra, which are normally taken at low spectral resolution owing to the extreme weakness of the signal levels. The vibrational term values of the B and C states given in Table 1 were used to generate the band locations shown in Fig. 1. The derived  $\omega_e$

**Table 2.** Relative transition probabilities for the NiO\* C  $^3\Sigma^-X^3\Sigma^-$  blue bands averaged over three spin sub-states.

$v'\backslash v''$	0	1	2	3	4	5	6	7	8	9	10	11	12
0	100	64	37	18	7	2	0	0	0	0	0	0	0
1	87	40	35	27	19	12	5	1	0	0	0	0	0
2	52	64	19	28	26	15	12	7	2	0	0	0	0
3	32	39	59	12	18	27	13	11	8	3	0	0	0
4	18	28	41	46	13	10	26	13	10	8	4	1	0
5	8	25	21	45	36	13	7	25	14	9	8	5	1
6	2	17	21	21	42	31	10	6	23	14	9	8	5
7	0	8	22	16	24	36	30	7	7	22	13	9	8
8	0	2	13	22	13	27	29	29	5	8	21	12	9
9	0	0	4	18	19	12	28	23	27	3	9	22	11
10	0	0	0	7	21	16	13	28	18	25	2	9	22
11	0	0	0	0	10	23	14	14	28	14	22	2	10
12	0	0	0	0	1	12	24	12	14	27	11	19	1

values, 587 and 605  $\text{cm}^{-1}$ , for the two systems are very similar in value to  $\omega' = 590 \text{ cm}^{-1}$  obtained by Malet and Rosen [11] for their Systems IV and V. The present analysis tentatively assumes  $^3\Sigma^-X^3\Sigma^-$  transitions for the two states; this is partly based on the spin state assignments of Srdanov and Harris [7]. Rotational constants for the three spin states are determined from high-resolution laboratory observations and are recorded in Table 1, identified as the B  $^3\Sigma$  and C  $^3\Sigma$  upper states. The three derived  $B_0$  values are approximately the same for the B  $^3\Sigma$  and C  $^3\Sigma$  states.

Another NiO band system, the  $^3\Sigma^-X^3\Sigma^-$  transition occurring in the red spectral region [9], is included here as it is also expected to be present in the night airglow spectrum. Friedman-Hill and Field [9] clearly identify transitions in each of the three spin states;  $0e$ ,  $1e$ , and  $1f$ . Preliminary constants have been determined from the Friedman-Hill and Field [9] detailed tabulations and are included in Table 1, column Red A  $^3\Sigma^-$ . Each of the three  $B_0$  constants are listed for reference and are included in the model calculations of the rotational branches. An estimate of the spin splitting in the upper state is also included; this is also based on the Friedman-Hill and Field [9] tabulations. From their analysis of the 0-0, 1-0, and 2-0 bands, a tentative model of the band positions and the spectral profiles of the dominant P and R branches in each band has been constructed.

Further into the infrared, the  $^3\Sigma^-X^3\Pi$  NiO\* band system has been positively identified by Friedman-Hill and Field [9], with a transition system origin at approximately 11780  $\text{cm}^{-1}$ . This system is outside the range of interest for the current analysis and so is not included here.

Relative line strengths for the rotational lines in the R and P branches of NiO\* are also required for the construction of the model spectra. As a first approximation, the classical Hönl-London values [12] are assumed. These are verified through comparison with the rotationally resolved spectra obtained by Srdanov and Harris [7], Friedman-Hill and Field [9], and Balfour et al. [8].

For this preliminary study, the isotopic components are ignored in the model simulations. The natural  $^{58}\text{Ni}$ - $^{60}\text{Ni}$  ratio is large, approximately 3 : 1, but the isotopic shifts are only a few wavenumbers; this is small compared with the spectral resolution of typical night airglow observations of very weak emissions.

The molecular constants listed in Table 1 provide the basis for calculating individual NiO\* band locations and emission spectral profiles of the various  $v'$  progressions. Techniques for determining relative band intensities in the simulations are addressed in the next section.

## 2.2 Franck-Condon factors and transition probabilities

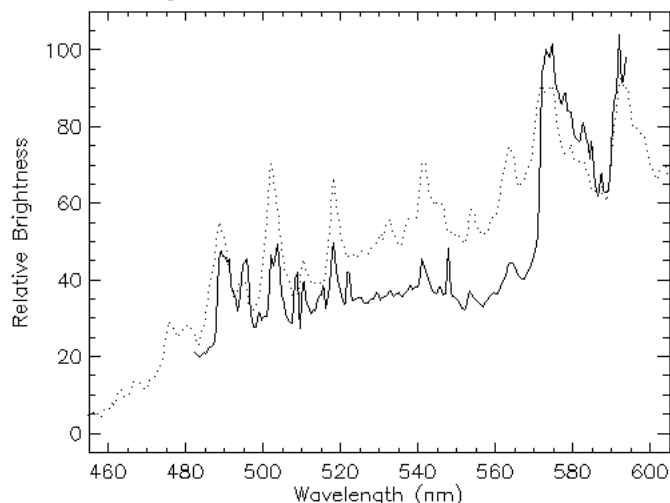
Estimates of relative band intensities within a band system are commonly based on calculated Franck-Condon factors. For the NiO\* band systems these factors do not appear to be available. However, the calculations can be performed using the spectral constants in Table 1 with the caveat that the uncertainty in the spectral constants will necessarily lead to uncertainties in the Franck-Condon factors. In the present study, the Franck-Condon factors were calculated using an adaptation of the FORTRAN code provided by Telle and Telle [13]. Sample program output was checked against known band systems for other molecules to validate the implementation of the algorithms.

The relative intensities of bands in  $v'$  progressions are defined according to the Franck-Condon factors. Similarly, using the factors from different  $v'$  levels the relative populations in each level can be determined through an iterative comparison between the model and an observed spectrum, as described in the next section.

The rotational constant,  $B_0$ , is different for each of the branch subsets associated with a spin state transition (Table 1), therefore, the calculated Franck-Condon factors will also vary. In this study, the Franck-Condon factors, expressed as relative transition probabilities [13] for each spin substate, are applied separately.

The calculated transition probabilities for the NiO\* C  $^3\Sigma^-X^3\Sigma^-$  blue bands, in this case normalized to 99 and averaged over the three spin sub-states, are listed in Table 2. The values in  $v'$  and  $v''$  progressions do not generally follow smoothly varying changes. Because, as mentioned above, the constants from Table 1 are preliminary values, it is expected that individual transition probabilities in Table 2 might be different in a more precise model. The relative transition probabilities for the other NiO\* band systems included in the model are not tabulated here, but the general pattern with  $v'$  and  $v''$  in each case is similar to the C  $^3\Sigma^-X^3\Sigma^-$  transition.

**Fig. 2.** A comparison of the NiO\* laboratory observations by Srdanov and Harris [7] (solid) and Burgard et al. [15] (dot) over the 460–600 nm spectral range. The two datasets are arbitrarily normalized for the comparison.

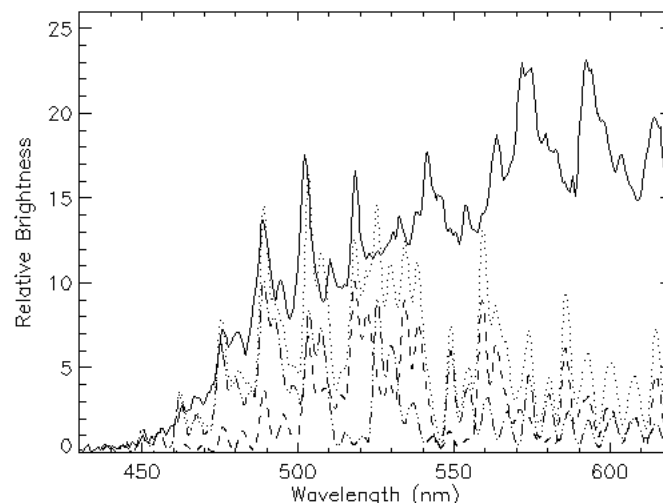


In addition to the model constraints on band intensities imposed by the Franck–Condon factors, the energy limitations of (1) must also be considered. Using the value of  $373 \pm 3$  kJ/mol for the bond energy of NiO [14], the energy balance of the reaction is +266 kJ/mol, or  $22236 \text{ cm}^{-1}$  [2]. The corresponding wavelength threshold for emission from the NiO\* product is approximately 440 nm. For the blue systems this places the highest attainable upper vibrational level at approximately  $v' = 7$ , while for the red system  $v' = 12$  is possible. The simulations described in the next section are constrained by these limits.

### 3. The NiO\* band model – comparison with chemiluminescent NiO\* observations

The emphasis here is on using low-resolution laboratory observations of NiO\* chemiluminescent emission spectra as a reference to determine the relative intensities of bands and systems within the NiO\* model. The two laboratory observations of the chemiluminescent NiO\* spectrum most useful in this study are those of Srdanov and Harris [7] and Burgard et al. [15]. In Fig. 2, the two observed spectra are compared over the common spectral range. Both spectra are expressed here in relative photon units; in addition, the Srdanov and Harris [7] spectrum has been corrected for the relative wavelength response of the 1P21 photomultiplier detector. This procedure assumes that the optical transmission is flat over the wavelength range of the Srdanov and Harris [7] spectrum. The NiO\* emission source used by Srdanov and Harris [7] was an Ni–O<sub>3</sub> mixture, which is directly relevant to the atmosphere, while Burgard et al. [15] used an Ni(CO)<sub>4</sub>–CO mixture in an O<sub>2</sub>–O<sub>3</sub> mixture [16]. The two spectra in Fig. 2 are very similar. As the spectrum by Burgard et al. [15] covers the wavelength range from the ultraviolet to the infrared, because the relative spectral calibration is known, and because the Ocean Optics 65000 spectrometer has a flat response over the wavelength range of the NiO\* spectrum, it has been chosen as the laboratory “standard” for NiO\* emission in this preliminary study.

**Fig. 3.** A comparison between the NiO\* laboratory observations of Burgard et al. [15] (solid) and the model simulations for the B  $^3\Sigma^-$ –X  $^3\Sigma^-$  (dash) and C  $^3\Sigma^-$ –X  $^3\Sigma^-$  (dot-dot-dash) systems and the model sum (dot).



To simplify the analysis, the comparison between the model spectra and the laboratory spectrum has been conducted in incremental stages. The initial comparison in Fig. 3 includes only the two blue band systems, B  $^3\Sigma^-$ –X  $^3\Sigma^-$  and C  $^3\Sigma^-$ –X  $^3\Sigma^-$ , in the model simulation. Relative  $v'$  populations are determined iteratively, as described above and constrained by the calculated Franck–Condon factors. This procedure uses an initial visual comparison followed by a minimization of the least squares difference. The two model systems are best simulated with the largest population in  $v' = 0$ , decreasing linearly by a factor of ten to  $v' = 7$ . The model matches many of the observed features in the blue region, including the rapid taper towards zero in the 450 nm region. As expected, the two model band systems do not explain the observed spectrum in the red region.

The next stage in the comparison is shown in Fig. 4, this time with the A  $^3\Sigma^-$ –X  $^3\Sigma^-$  band system added to the model simulation. The match with the observed band features in the 600–650 nm region is improved compared to Fig. 3. In the A  $^3\Sigma^-$  upper state the  $v'$  distribution is assumed to be approximately uniform from  $v' = 0$  to  $v' = 7$  with a taper to nearly zero by  $v' = 10$ ; again this distribution is based on the iterative fit. However, much of the emission observed in the comparison in Fig. 4 remains unexplained.

To address the observed features that are missing in the model spectrum in Fig. 4 an unidentified band system is postulated: the D(?)–X  $^3\Sigma^-$  system. We have tentatively labeled the upper state D, although the assigned energy is below the currently assigned A-state energy. There are prominent spectral features observed in the laboratory spectrum at 573, 593, 615, 673, and 714 nm that are not matched by the known band systems. An airglow feature at 714 nm has previously been reported by McDade et al. [17], and confirmed by Slanger et al. [18], has been attributed to the O<sub>2</sub> (b-X) atmospheric (4–3) band. However, the infrequent appearance of NiO\* emission makes it unlikely that the McDade et al. [17] observations are due to NiO\*. Approximate electronic and vibrational term values have been esti-

**Fig. 4.** A comparison between the NiO\* laboratory observations of Burgard et al. [15] (solid) and the model simulation of the A  $^3\Sigma^- - X^3\Sigma^-$  system (dash) with the sum of the blue B  $^3\Sigma^- - X^3\Sigma^-$  and C  $^3\Sigma^- - X^3\Sigma^-$  systems and the red system (A  $^3\Sigma^- - X^3\Sigma^-$ ) (dotted).

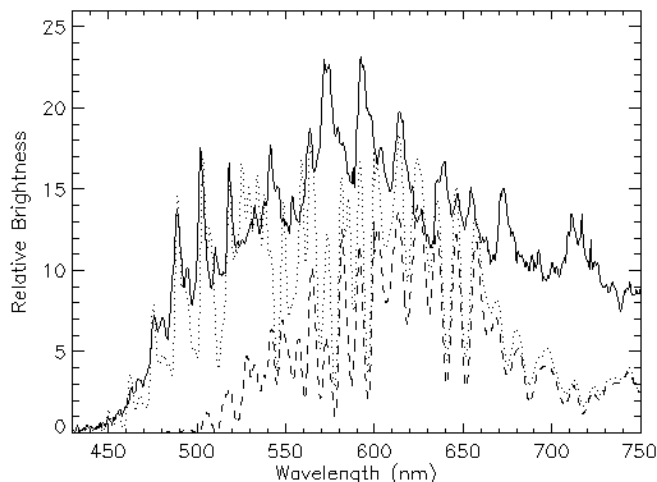
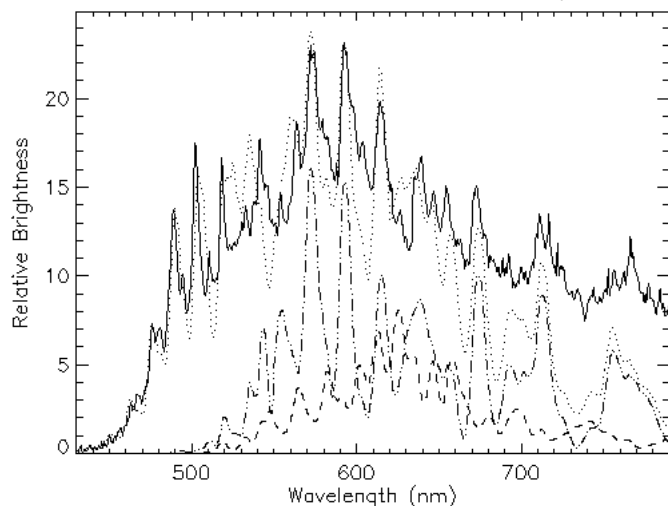


**Fig. 5.** A comparison between the NiO\* laboratory observations of Burgard et al. [15] (solid) and the model simulations for the red A  $^3\Sigma^- - X^3\Sigma^-$  system (dash) and the new D(?)  $- X^3\Sigma^-$  system (dot-dot-dash). The model sum (dot) includes the four band systems.



mated to simulate the observed locations (Table 1, New D(?)). The simulated D(?)  $- X^3\Sigma^-$  system is added to the total model spectrum in Fig. 5. The assumed vibrational populations in the D(?) state are approximately uniform from  $v' = 0$  to  $v' = 5$  and then taper to zero by  $v' = 9$ , similar to the A  $^3\Sigma^-$  distributions shown in Fig. 4. In this case, the D(?) state vibrational populations are simply assumed. With the addition of the D(?)  $- X^3\Sigma^-$  system, the relative contribution from the A  $^3\Sigma^- - X^3\Sigma^-$  system is reduced.

The relative contribution from each of the four band systems included in the simulation in Fig. 5 is uniform within a factor of two, the D(?)  $- X^3\Sigma^-$  system being the brightest and the A  $^3\Sigma^- - X^3\Sigma^-$  being the weakest.

Only comparisons between the model and NiO\* chemiluminescent emissions at laboratory pressures are included here. As noted by Evans et al. [2], the short-wave spectral

cutoff at much lower mesospheric pressures is extended towards the blue end of the spectrum by as much as 15 nm; the result of increased populations in higher vibrational levels in the upper electronic states. As relative vibrational populations are free parameters in the band system models described here, this furthers the need for study of various excitation processes.

#### 4. Conclusion

High spectral resolution laboratory observations of NiO transitions have been reviewed and approximate molecular constants determined for three band systems. These constants form the basis for a spectral simulation model of the rotational line and band positions for the measured electronic transitions, all connected to the NiO ground state. As the detailed observational data are limited to only a few bands in each case, the molecular constants must be considered preliminary.

The chemiluminescent NiO\* emission spectrum obtained from independent laboratory observations has been reviewed and shown to be repeatable. One of the observed spectra was chosen as the reference observed spectrum and, through an iterative process, simulated spectra of the three known band systems were adjusted to match the observed NiO\* “reference” spectrum. Band intensities were determined and, combined with tables of approximate relative transition probabilities, vibrational distributions in the upper excited states have been inferred.

The fit between the laboratory spectrum and the model spectrum using only the three known band systems is inadequate. Through an iterative procedure, the molecular constants for a postulated new band system have been determined. This new system simulates a number of prominent observed spectral features that are not matched by the known band systems. Detailed laboratory observations are required to identify this new NiO band system unambiguously.

The developed simulation model is intended to be used to assist in the identification of faint NiO\* chemiluminescent emissions in the night airglow. Further laboratory studies of the NiO\* spectrum at low pressure will add to the knowledge of the spectral shape of yet another emission species and so enhance the ability to study the spatial and temporal variation in airglow emissions.

#### Acknowledgments

The authors wish to thank an anonymous referee for the excellent suggestions that have greatly improved the manuscript. This work has been supported through Grants from the Natural Sciences and Engineering Research Council of Canada.

#### References

1. W.F.J. Evans, R.L. Gattinger, T.G. Slanger, D.V. Saran, D.A. Degenstein, and E.J. Llewellyn. *Geophys. Res. Lett.* **37**, L22105 (2010). doi:10.1029/2010GL045310.
2. W.F.J. Evans, R.L. Gattinger, A.L. Broadfoot, and E.J. Llewellyn. *Atmos. Chem. Phys. Discuss.* **11**, 11839 (2011). doi:10.5194/acpd-11-11839-2011.
3. H. Brown and C. Patterson. *J. Geol.* **55**, 508 (1947). doi:10.1086/625461.

4. L.S. Schramm, D.E. Brownlee, and M.M. Wheelock. *Meteoritics*, **24**, 99 (1989).
5. C.S. Gardner, J.M.C. Plane, W. Pan, T. Vondrak, B.J. Murray, and X. Chu. *J. Geophys. Res.* **110**, D10, D10302 (2005). doi:10.1029/2004JD005670.
6. R.L. Gattinger, W.F.J. Evans, D.A. Degenstein, and E.J. Llewellyn. *Can. J. Phys.* **89**, 239 (2011). doi:10.1139/P11-003.
7. V.I. Srdanov and D.O. Harris. *J. Chem. Phys.* **89**, 2748 (1988). doi:10.1063/1.455711.
8. W.J. Balfour, J. Cao, R.H. Jensen, and R. Li. *Chem. Phys. Lett.* **385**, 239 (2004). doi:10.1016/j.cplett.2003.12.089.
9. E.J. Friedman-Hill and R.W. Field. *J. Mol. Spectrosc.* **155**, 259 (1992). doi:10.1016/0022-2852(92)90516-Q.
10. B. Rosen. *Nature*, **156**, 570 (1945). doi:10.1038/156570a0.
11. M. Malet and B. Rosen. *Bull. Soc. Roy. Sci. Liege*, **14**, 382 (1945).
12. G. Herzberg. *Molecular spectra and molecular structure I. Spectra of diatomic molecules*. Van Nostrand, Princeton, NJ, 1950.
13. H.H. Telle and U. Telle. *Comput. Phys. Commun.* **28**, 1 (1982). doi:10.1016/0010-4655(82)90059-5.
14. L.R. Watson, T.L. Thiem, R.A. Dressler, R.H. Salter, and E. Murad. *J. Phys. Chem.* **97**, 5577 (1993). doi:10.1021/j100123a020.
15. D.A. Burgard, J. Abraham, A. Allen, J. Craft, W. Foley, J. Robinson, B. Wells, C. Xu, and D.H. Stedman. *Appl. Spectrosc.* **60**, 99 (2006). doi:10.1366/000370206775382730.
16. D.H. Stedman, D.A. Tamaro, D.K. Branch, and R. Pearson. *Anal. Chem.* **51**, 2340 (1979). doi:10.1021/ac50050a012.
17. I.C. McDade, E.J. Llewellyn, R.G.H. Greer, and D.P. Murtagh. *Planet. Space Sci.* **34**, 801 (1986). doi:10.1016/0032-0633(86)90076-0.
18. T. Slanger, P. Cosby, D. Huestis, and D. Osterbrock. *J. Geophys. Res.* **105**, D16, 20557 (2000). doi:10.1029/2000JD900256.